and more generally

$$V = av_w + b \tag{7'}$$

where the term $a = A/A_w = (V/v_w)_{CH_2}$ approximately is 1.6.

In eq 7′ the volume v_w appears indeed multiplied by a factor larger than unity, as if the impenetrable volume were larger than van der Waals volume, presumably because of intrinsic geometrical factors.

Therefore, the term $b = V - av_w$ may be identified with the volume really involved in interactions for all compounds containing a given functional group and it is constant along a series.

Reasonably all these conclusions are meaningful only in the limits of validity of the linear dependence on the number of CH_2 groups in the molecule of quantities which appear in eq 3-6.

Empirical equations like eq 7′ were found by previous authors (*3*, *4*) to be useful in reproducing experimental data in the case of series of homologous substances: cyclic and acyclic alcohols, ethers, ketones, diols, amines, etc.

In Tables VIII and IX the parameters of linear correlation A, B, a, and b are reported. For the sake of homogeneity the analysis is limited to the first four or five members of each homologous series, which are liquid in the standard state. As expected, the term a may be regarded as a constant, for both pure substances and dilute aqueous solutions. It reflects the constant contributions of CH_2 groups to $V°$, $\bar{v}_2$, and v_w. The term b on the contrary, is characteristic of each series, involving the effects of the functional group present in the molecule responsible for interactions. Therefore, the magnitude of the term b, as well as its change from a solvent to another, might be indicated as a criterion for detecting the extent of interactions of any kind and evidencing the structure-making or -breaking solvent effect.

As a general rule a shrinkage is indeed evidenced in transferring 1 mol of substance from pure state to a dilute aqueous solution according to the above-quoted water effects on polar solutes. Diols seem to be an exception since the term b is larger for water solutions (5.212) than for pure substances (4.512). This behavior is only apparently anomalous. The increase of the term b in aqueous solutions may well be ascribed to the destruction by water of hydrogen bonds between OH groups present in diol molecules, which counterbalance in excess the effects of interactions of diols with water.

Acknowledgment

We are indebted to Luigi Lisbo Parrella for technical assistance.

Registry No. CH_3CN, 75-05-8; CH_3CH_2CN, 107-12-0; $CH_3(CH_2)_2CN$, 109-74-0; $CH_3(CH_2)_3CN$, 110-59-8; $CH_3(CH_2)_4CN$, 628-73-9; $CH_3(CH_2)_6CN$, 124-12-9.

Literature Cited

(1) Jannelli, L.; Pansini, M.; Jalenti, R. *J. Chem. Eng. Data*, previous paper in this issue.
(2) Jalenti, R.; Lopez, A.; Azzi, A. *Thermochim. Acta* **1980**, *35*, 315.
(3) Teresawa, S.; Itsuki, A.; Arakawa, S. *J. Phys. Chem.* **1975**, *79*, 2345.
(4) Edward, J. T.; Farrell, P. G.; Shahidi, F. *J. Chem. Soc., Faraday Trans.* **1977**, *73*, 705, 715.
(5) Nitta, T.; Turex, E. A.; Greenkorn, R. A.; Chao, R. C. *AIChE J.* **1971**, *23*, 144.
(6) Lopez, A.; Jannelli, L.; Silvestri, S. *J. Chem. Eng. Data* **1982**, *27*, 183.
(7) Riddick, A. J.; Bunger, W. B. "Organic Solvents", 3rd ed.; Wiley-Interscience: New York, 1970.
(8) Jannelli, L.; Lopez, A.; Saiello, S. *J. Chem. Eng. Data* **1980**, *25*, 259.
(9) Cabani, S.; Conti, G.; Lepori, L. *J. Phys. Chem.* **1972**, *76*, 1338; **1974**, *78*, 1930.
(10) Millero, F. J. "Water and Aqueous Solutions"; Horne, R. A., Ed.; Wiley-Interscience: New York, 1972; pp 519, 566.
(11) Bondi, A. *J. Phys. Chem.* **1984**, *68*, 441.
(12) Alexander, M. *J. Chem. Eng. Data* **1959**, *4*, 252.
(13) Treszczanowicz, A. J.; Kiyohara, O.; Benson, G. C. *J. Chem. Thermodyn.* **1981**, *13*, 253.
(14) "Handbook of Chemistry and Physics", 58th ed.; CRC Press: Cleveland, OH 44128, 1977-78.

Received for review June 28, 1983. Accepted November 28, 1983.

Binary Vapor–Liquid Equilibria of Carbon Dioxide with 2-Methyl-1-pentene, 1-Hexene, 1-Heptene, and *m*-Xylene at 303.15, 323.15, and 343.15 K

Juan H. Vera* and Hasan Orbey

Department of Chemical Engineering, McConnell Engineering Building, McGill University, Montreal, PQ, Canada H3A 2A7

Binary vapor–liquid equilibrium data at 303.15, 323.15, and 343.15 K for the systems CO_2–2-methyl-1-pentene, CO_2–1-hexene, CO_2–1-heptene, and CO_2–*m*-xylene measured in a static equilibrium cell are presented. The data were correlated by using the Peng–Robinson equation of state. The Peng–Robinson equation represents tha data well at all temperatures.

Introduction

Increased interest in tertiary oil recovery by carbon dioxide flooding, and extraction of coal as well as natural products by carbon dioxide, has encouraged studies of vapor–liquid equilibrium of carbon dioxide and unsaturated/aromatic hydrocarbon systems. Carbon dioxide–unsaturated hydrocarbon systems were previously neglected since they are not of primary importance to the petroleum industry, for which early carbon dioxide–hydrocarbon data were collected.

In this work, vapor–liquid equilibrium data are reported for the binary systems CO_2–2-methyl-1-pentene, CO_2–1-hexene, CO_2–1-heptene, and CO_2–*m*-xylene at 303.15, 323.15, and 343.15 K over a pressure range of 0–7.5 MPa. The data are reduced with the Peng–Robinson (*1*) equation of state. Temperature-independent parameters that allow interpolation of data are obtained.

Experimental Section

A schematic diagram of the apparatus is shown in Figure 1. The central unit was a blind, stainless-steel, constant-volume cell with an internal capacity of about 250 cm^3. The degassed

0021-9568/84/1729-0269$01.50/0

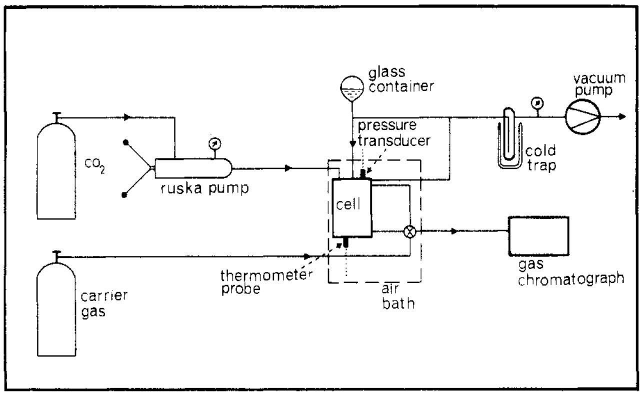

Figure 1. Schematic diagram of the apparatus.

Table I. Columns Used in Gas-Chromatographic Analyses

system	column	column temp, K
CO_2-*m*-xylene	3 m, 3-mm o.d. 7.5% Carbowax on 40/60 mesh Chromosorb T	393
CO_2-2-methyl-1-pentene		323
CO_2-1-hexene	3 m, 3-mm o.d. 10% polyphenyl ether on 80/100 mesh Chromosorb	323
CO_2-1-heptene		353

liquid component was injected into the cell from a glass container by the action of gravity. The CO_2 gas was fed into the cell from a gas tank. A hand-operated Ruska Model 2200 positive displacement pump was connected to the gas line to make charging possible when the pressure of the cell was higher than that of the gas tank. To maintain the desired temperature, the cell and its immediate auxiliaries were placed in a constant-temperature air bath. The bath was heated by means of an externally located 500-W heater-blower assembly. The bath temperature was controlled by a Versatherm solid-state controller unit. Equilibrium in the cell was attained by using a magnetic stirrer coupled to an external rotating magnet. Equilibrium pressure was measured by means of a Dynisco PT422A, 0-1500 psi strain gauge pressure transducer. The transducer was calibrated with a Chandler dead-weight tester. This allowed the pressure to be known to about ±0.2% full scale. The temperature in the cell was measured by a Hewlett-Packard quartz thermometer, Model 2801A, with Model 2850C-111-25 probe. This instrument was capable of providing ±0.05 K accuracy.

In order to sample the vapor and the liquid phases, two specially designed custom-made valves were placed into the cell body. The design of these valves was similar to that described by Kalra et al. (*2*). A sampling valve consisted of a four-port valve housing protruding into the cell. Two opposite holes of the housing were connected to a sampling loop, and the other two were exposed directly into the cell. A stainless-steel sampling rod, bored with a hole horizontally along a diameter of the rod near the tip, was mounted through packing into the valve housing in such a way that the hole in the rod was aligned with the ports of the housing. By 90° rotations of the rod, a small amount of gas or liquid was trapped in the rod and transferred into the sampling loop. Helium was then passed through the sampling loop to sweep the sample into a gas chromatograph.

For determination of phase compositions a Hewlett-Packard 5730A gas chromatograph with 3380A integrator was used. A thermal conductivity detector was employed in all cases. Column used and operating conditions are summarized in Table I. The gas chromatotgraph was calibrated by using pure components. Compositions were calculated by using a response factor method similar to that described by Smith and Bowden (*3*). For each data point two or more samples were taken. The maximum combined error in phase composition determinations was estimated to be 0.7 mol %.

Table II. Equilibrium Phase Properties of the CO_2-2-Methyl-1-pentene System

press., MPa	x_{CO_2}	y_{CO_2}	press., MPa	x_{CO_2}	y_{CO_2}
		$T = 303.15$ K			
1.020	0.157	0.962	4.070	0.651	0.992
2.020	0.318	0.988	4.780	0.759	0.991
2.695	0.428	0.983	5.490	0.830	0.993
3.390	0.562	0.990			
		$T = 323.15$ K			
1.280	0.161	0.938	4.540	0.526	0.977
2.015	0.243	0.963	5.410	0.614	0.977
2.725	0.322	0.969	6.145	0.705	0.984
3.250	0.379	0.974	7.430	0.848	0.978
		$T = 343.15$ K			
1.020	0.083	0.882	4.305	0.373	0.956
1.540	0.132	0.917	5.160	0.469	0.957
2.030	0.179	0.937	6.175	0.585	0.957
2.729	0.246	0.948	7.200	0.708	0.970
3.400	0.301	0.956			

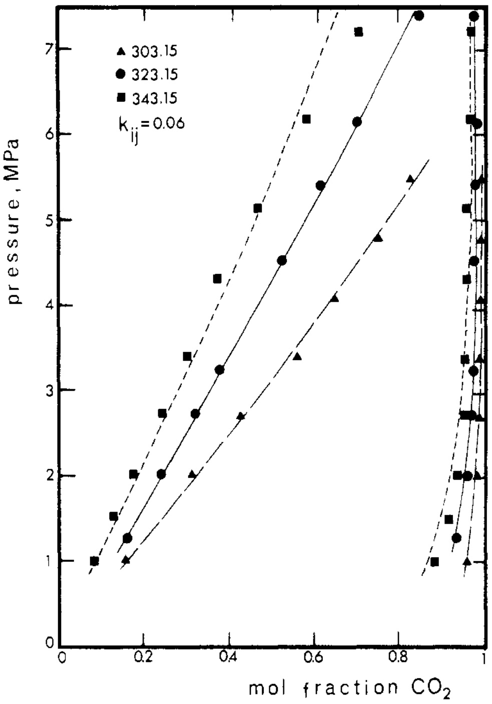

Figure 2. Pressure-equilibrium phase composition diagram for the CO_2-2-methyl-1-pentene system.

An auxiliary vacuum unit consisting of a nitrogen cold trap and an Alcatel Model 2008 vacuum pump was used to clean the cell, the charge lines, and the sampling loop prior to experimental runs.

All liquid chemicals were supplied by Aldrich Chemical Co. at a guaranteed purity of 99 mol %. Their chromatographic analyses indicated that the actual purity of the chemicals was better than 99.9 mol %. Carbon dioxide was supplied by Liquid Carbonic Canada Co., with a purity of 99.99 mol %. The chemicals were used without further purification. Only degassing of liquid chemicals was performed prior to the experiments.

Table III. Equilibrium Phase Properties of the CO_2-1-Hexene System

press., MPa	x_{CO_2}	y_{CO_2}	press., MPa	x_{CO_2}	y_{CO_2}
$T = 303.15$ K					
1.000	0.156	0.966	4.370	0.668	0.989
2.025	0.306	0.967	5.085	0.754	0.989
2.725	0.406	0.986	5.611	0.818	0.990
3.385	0.521		5.905	0.851	0.983
$T = 323.15$ K					
0.995	0.105	0.934	4.475	0.486	0.968
1.530	0.158	0.942	5.665	0.617	0.971
2.045	0.207		6.305	0.705	0.981
2.720	0.278	0.963	6.525	0.741	0.976
3.390	0.353	0.964			
$T = 343.15$ K					
1.030	0.082	0.899	3.390	0.283	0.947
1.535	0.117	0.912	4.490	0.376	0.946
2.015	0.158	0.927	5.370	0.476	0.951
2.735	0.216	0.944	6.020	0.541	0.955

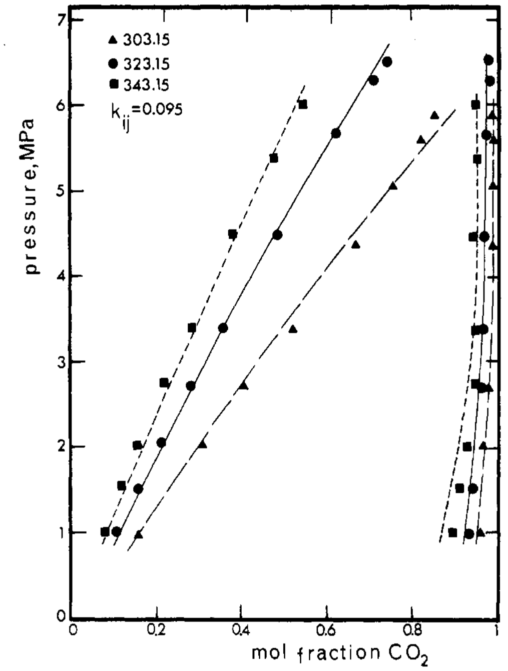

Figure 3. Pressure-equilibrium phase composition diagram for the CO_2-1-hexene system.

The experimental techniques are described in detail elsewhere (*4*).

Results and Discussion

The isothermal pressure-phase composition data for four systems studied in the work are tabulated in Tables II-V and are also presented in graphical form in Figures 2-5

The cubic equation of state of Peng-Robinson was used to correlate the data. The equation of state has the form

$$P = \frac{RT}{v - b} - \frac{a(T)}{v(v + b) + b(v - b)} \qquad (1)$$

with the following mixing rules

$$b = \sum_i x_i b_i \qquad (2)$$

$$a = \sum_i \sum_j x_i x_j a_{ij} \qquad (3)$$

where

$$a_{ij} = (a_i a_j)^{0.5}(1 - k_{ij}) \qquad i \neq j \qquad (4)$$

Table IV. Equilibrium Phase Properties of the CO_2-1-Heptene System

press., MPa	x_{CO_2}	y_{CO_2}	press., MPa	x_{CO_2}	y_{CO_2}
$T = 303.15$ K					
1.020	0.157	0.990	3.725	0.564	0.992
1.510	0.217	0.993	4.730	0.675	0.995
2.055	0.292	0.995	5.590	0.803	0.995
2.910	0.435	0.993			
$T = 323.15$ K					
1.010	0.098	0.981	3.595	0.368	0.986
1.530	0.141	0.982	4.555	0.484	0.986
2.035	0.206	0.983	5.470	0.584	0.987
2.915	0.300	0.984	6.275	0.676	0.985
$T = 343.15$ K					
1.010	0.074	0.958	4.265	0.364	0.976
1.530	0.114	0.956	5.290	0.455	0.976
2.045	0.158	0.961	6.090	0.533	0.980
2.720	0.206	0.972	7.315	0.704	0.981
3.700	0.300	0.974			

Table V. Equilibrium Phase Properties of the CO_2-*m*-Xylene System

press., MPa	x_{CO_2}	y_{CO_2}	press., MPa	x_{CO_2}	y_{CO_2}
$T = 303.15$ K					
0.670	0.077	0.995	2.705	0.304	0.997
1.305	0.148	0.996	3.305	0.375	0.996
2.010	0.235	0.996			
$T = 323.15$ K					
0.675	0.076		2.690	0.247	0.995
1.600	0.147	0.993	3.335	0.323	0.994
2.680	0.238	0.995			
$T = 343.15$ K					
1.620	0.106	0.986	2.700	0.189	0.991
2.335	0.157	0.991	3.520	0.247	0.992
2.715	0.174	0.990			

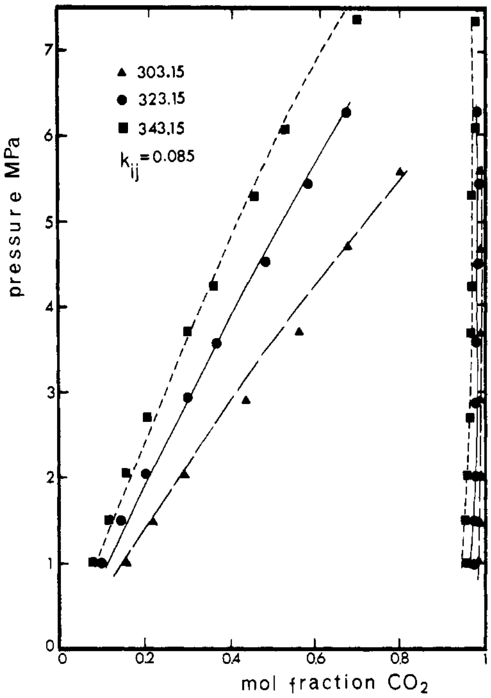

Figure 4. Pressure-equilibrium phase composition diagram for the CO_2-1-heptene system.

The interaction parameters k_{ij} were evaluated for the systems presented in this work except for the system of CO_2-*m*-xylene, for which k_{ij} has been reported by Ng et al. (*5*). The criterion used for the evaluation of k_{ij} values was the mini-

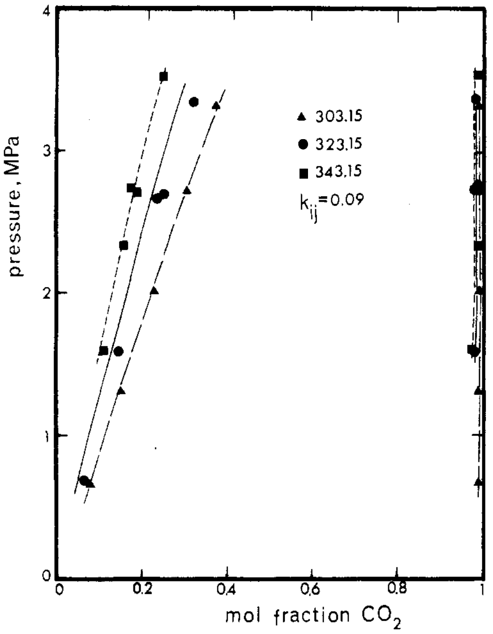

Figure 5. Pressure-equilibrium phase composition diagram for the CO_2–*m*-xylene system.

mization of the percent error in the calculated total pressure. Values of k_{ij} obtained and estimation of the data by the Peng–Robinson equation of state are also presented in Figures 2–5. A fairly good representation of the data by the Peng–Robinson equation was achieved.

While this work was in progress, Ng et al. (*5*) published a study reporting data for the system CO_2–*m*-xylene. Some of these data were in the same temperature and pressure range as those previously measured in this work. Although the isotherms do not match exactly, the compatibility of the two sets of data is good. The estimation of CO_2–*m*-xylene data measured in this work using the k_{ij} values reported by Ng et al. was good except for the 323.15 K isotherm, for which estimated pressures were always larger than the experimental values. Data for the system CO_2–*m*-xylene at higher temperatures are available in the literature (*6*).

Glossary

P	pressure
R	universal gas constant
T	temperature
v	molar volume
a, *b*	parameters in Peng–Robinson equation of state
k	binary interaction parameter
x	mole fraction in liquid phase
y	mole fraction in vapor phase

Subscripts

i, j	components

Registry No. CO_2, 124-38-9; 2-methyl-1-pentene, 763-29-1; 1-hexene, 592-41-6; 1-heptene, 592-76-7; *m*-xylene, 108-38-3.

Literature Cited

(1) Peng, D.-Y.; Robinson, D. B. *Ind. Eng. Chem. Fundam.* **1976**, *15*, 59–64.
(2) Kalra, H.; Kubota, H.; Robinson, D. B.; Ng, H.-J. *J. Chem. Eng. Data* **1978**, *23*, 317–21.
(3) Smith, B. D.; Bowden, W. W. *Anal. Chem.* **1964**, *36*, 87–9.
(4) Orbey, H. Ph.D. Thesis, McGill University, Montreal, Canada, 1983.
(5) Ng, H.-J.; Huang, S. S.-S.; Robinson, D. B. *J. Chem. Eng. Data* **1982**, *27*, 119–22.
(6) Sebastian, H. M.; Simnick, J. J.; Lin, H.-M.; Chao, K.-C. *J. Chem. Eng. Data* **1980**, *25*, 246–8.

Received for review April 21, 1983. Accepted November 29, 1983. The financial support received from NSERC, Canada, is gratefully acknowledged.

Three-Phase Liquid–Liquid–Vapor Equilibria in the Methane + *n*-Hexane + Nitrogen and Methane + *n*-Pentane + Nitrogen Systems

Robert C. Merrill, Jr.,[†] **Kraemer D. Luks,**[‡] **and James P. Kohn***
Department of Chemical Engineering, University of Notre Dame, Notre Dame, Indiana 46556

The phase behavior of two ternary systems (methane + *n*-hexane + nitrogen, methane + *n*-pentane + nitrogen) in their three-phase liquid–liquid–vapor (L_1–L_2–V) regions is presented, with specific attention paid to the nature of the boundaries of the regions. Liquid-phase compositions and molar volumes are reported as functions of temperature and pressure, both within the three-phase regions and at the boundaries. The methane + *n*-hexane + nitrogen system has a L_1–L_2–V region bounded by a Q-point (S–L_1–L_2–V) locus, a K-point (L_1–L_2 = V) locus, an LCST (L_1 = L_2–V) locus, and the binary methane + *n*-hexane L_1–L_2–V locus. The methane + *n*-pentane + nitrogen system's L_1–L_2–V region is bounded by Q-point, K-point, and LCST loci.

Introduction

We have undertaken an extensive study of liquid–liquid–vapor (L_1–L_2–V) phenomena in well-defined ternary prototype systems of liquefied natural gas (LNG). Previously, we have studied six ternary systems (*1–3*) composed of methane (solvent) plus *n*-octane (solute) with the following second solvents as the third component: ethane, propane, *n*-butane, *n*-pentane, *n*-hexane, and carbon dioxide. We also studied the system (*3*) methane *n*-hexane with carbon dioxide as the second solvent. In classifying these systems, we made special note of the nature of the boundaries of the L_1–L_2–V thermodynamic phase space. These spaces could be bounded by loci of (1) K points (L_1–L_2 = V), (2) LCST points (L_1 = L_2–V), (3) Q points (S–L_1–L_2–V), and (4) the methane + *n*-hexane binary L_1–L_2–V behavior, when applicable. The LCST and K-point loci can intersect as a tricritical point (L_1 = L_2 = V). In some of these ternary systems it should be recognized that the solute (e.g., *n*-octane) is not immiscible with either the primary or the secondary

---

[†] Present address: SOHIO Research Center, Cleveland, OH 44128.
[‡] Present address: Department of Chemical Engineering, University of Tulsa, Tulsa, OK 74104.

0021-9568/84/1729-0272$01.50/0